The Theory of Speckle Intensity Correlations Over Object Position in a Heavily Scattering Random Medium

Kevin J. Webb* and Qiaoen Luo

Purdue University, West Lafayette, IN 47907, USA

* *Corresponding author: webb@purdue.edu*

Abstract

We present a general theory for optical imaging of moving objects obscured by heavily scattering random media. Measurements involve collecting a series of speckle intensity images as a function of the position of a moving object. A statistical average intensity correlation can be formed with the potential to provide access to microscopic and macroscopic information about the object. For macroscopic objects and translation distances that are both large relative to the wavelength, there is a clear method to invert measurements to form an image of the hidden object. Opportunities exist for super-resolution sensing and imaging, with far-subwavelength resolution. Importantly, there is no fundamental limit to the thickness of the background randomly scattering medium, other than the practical requirement of detecting an adequate number of photons and sufficient background scatter for developed Gaussian field statistics. The approach can be generalized to any wave type and frequency, under the assumption that there is adequate temporal coherence. Applications include deep tissue *in vivo* imaging and sensing in and through various forms of environmental clutter. The theory also provides another dimension for intensity interferometry and entangled state detection to the case with motion of the scatterer or emitter.

I. INTRODUCTION

Electromagnetic waves are of broad consequence in the natural and engineered world. Notably, photonics is pervasive in communications, optical sensing, and imaging, providing capacity by virtue of the carrier frequency and the transmission media, and information through spectroscopy, leading to the expanding presence of optical methods in medical research and medicine. Throughout the application spaces in science and technology, random scatter generally presents difficulties. For example, atmospheric scatter has long limited earth-based astronomy. Tissue scatter of light has made high resolution coherent imaging *in vivo* a challenge at depths beyond a few hundred microns.

The scatter of coherent light from randomly arranged scatterers in bulk material or rough surfaces results in speckle, the granular intensity patterns from the interference between the wavefronts of the differently scattered fields, and if the scatterers move, the speckle pattern changes accordingly. Therefore, in principle, information about a scattering medium or the light impinging on such a medium is available. However, the challenge is to find a means to extract such information. Because of the difficulty associated with describing deterministic light propagation in the multiply-scattered regime, a statistical treatment becomes important [1]. Changes in speckle patterns are used in diffusing wave spectroscopy [2] and laser speckle contrast imaging [3], where motion reduces the local granular nature of the speckle pattern during the image collection window. The local speckle contrast ratio can thus be an indicator of the velocity of blood flow under thin skin [4]. Decreasing the temporal coherence (increasing the bandwidth of laser light) reduces the speckle contrast ratio (the ratio of the speckle intensity standard deviation to the mean), effectively reducing the graininess. There is therefore a relationship between speckle decorrelation over scanned frequency and the transport of light through the scattering medium [5, 6]. The ensemble-averaged temporal response of a random medium, useful in characterizing random media and imaging, can be obtained using third-order correlations of speckle patterns over frequency, thereby providing access to the Fourier phase, when the field is described by circular complex Gaussian statistics [6]. This implies the detection of polarized light and allows use of a moment theorem [7]. Control of the temporal coherence of the light source provides a means to image hidden objects [8]. Practically, fixing the light source while increasing the scatter also reduces the contrast ratio. Speckle contrast can be reduced by reducing spatial coherence using, for

example, random lasers, allowing full-field imaging [9]. Speckle intensity patterns can also be tailored to have artificial statistics, non-existing in naturally occurring speckle, using a spatial light modulator, and this has been considered for applications [10]. The presence of scatter can also increase communication capacity because of access to multiple independent channels [11, 12], as well as provide enhanced security [13, 14]. Characterization of the transmission properties or a random medium also allows access to the spectral properties of light incident on the scattering medium [15].

Imaging using coherent light offers high resolution, but increasing random scatter, such as occurs with biological tissue, eventually precludes direct observation. Consequently, coherent imaging of an object through a thick scattering medium is extremely difficult. The transmission of coherent light through a scattering medium has been studied intensely (see, for example, [5, 16, 17]). The memory effect (where the speckle pattern moves with the incident wave vector) [18] allows imaging through a scattering medium, as long as the thickness is small [18–22]. Wavefront control using a spatial light modulator and feedback control (based on a sensing arrangement at the point of interest) enables focusing through scatter [23, 24], facilitating point-wise imaging. Knowledge of the field transmission matrix (spatial point wise for the incident field) for a point within the scattering medium provides information that can be used to control the incident field (such as with a spatial light modulator) to focus at that point. The transmission matrix can be measured, but this requires sensing within or on the other side of the scattering medium or guidestar control of a small volume where the focus will occur [25–27]. The contrast has been directly related to the effective number of the contributing transmission matrix eigenchannels based on random matrix calculations [28]. While a challenging computational problem, inversion of measurement data can be presented as an estimation of the positions of a set of scatterers, and simplified using, for example, the first Born approximation describing the field scattered by each scatterer. Having this computational model for the background scattering medium would allow separation of measurement data when an object within or on the other side is to be imaged.

We develop a general statistical treatment that allows sensing and imaging of a moving object hidden inside a heavily scattering random background in a manner that is limited only by the number of photons detected. The imaging concept is presented in Fig. 1. Notably, the random background provides a structured field that also allows access to far-subwavelength

spatial information, along the lines of a proposal for super-resolution imaging with motion in prepared structured fields [29]. In this sense, the random scatter facilitates information that would otherwise be unavailable at a remote detector. The mathematical development generalizes earlier work showing the extraction of the incident field from correlations of intensity speckle patterns over translated field position [30, 31], the imaging of aperture-type objects between scattering slabs [32], and recent experimental evidence that general objects can be imaged [33]. The new theory provides a means to image and motivation for a series of experiments to evaluate new aspects of the the information that can be accessed.

We treat the moving object parameterization in the context of the wave equation in Sect. II. Intensity speckle patterns that can be measured as a function of object position are expanded as moments of the detected field in Sect. III. Section IV develops the relationship between the second order field moments and the object(s) to be imaged. The theory has short-range, subwavelength-scale information, and for macroscopic objects, information on the length scale commensurate with the object that can be used as a basis for sensing and imaging. Section V considers the physical basis of the normalized field correlation functions. The detector intensity correlation expression is developed in Sect. VI, where we arrive at a key relationship that is subsequently studied in Sect. VII in terms of length scale and the amount of the scatter from the moving object. The general theory is couched as a sensing and imaging methodology in Sect. VIII. Section IX presents a discussion of issues related to the theory, the experimental studies, and key applications, and Sect. X projects the potential impact in the form of a conclusion.

II. OBJECT PARAMETERIZATION

We treat the problem of imaging a moving object in a randomly scattering background medium (Fig. 1) as one where the background field without the object is considered as the incident field and the scattered field is that due to the object or objects of interest. This neglects possible displacement of background scatterers as the object of interest moves. Assuming a linear and locally time-invariant system during each measurement, the total field is exactly the superposition of the incident and scattered field everywhere. For scattering dielectric problems, it is convenient to use the electric field representation. The total field is $\mathbf{E} = \mathbf{E}_b + \mathbf{E}_s$, the sum of the background field ($\mathbf{E}_b$) and the scattered field ($\mathbf{E}_s$) due to the

moving object. Our interest here is in extracting information about the object from $\mathbf{E}_s$, but the challenge is that the associated field is heavily scattered by the background medium. Our treatment will use a Green's function for the wave equation that will remain unknown throughout the development.

The source-free Maxwell curl equations in the temporal frequency domain ($\exp(-i\omega t)$) and for non-magnetic media are

$$\nabla \times \mathbf{H} = -i\omega\epsilon_0\epsilon\mathbf{E} \tag{1}$$

$$\nabla \times \mathbf{E} = i\omega\mu_0\mathbf{H}, \tag{2}$$

where we have assumed that a complex, isotropic dielectric constant $\epsilon(\mathbf{r})$ describes the scattering problem, and $\mathbf{H}$ is the magnetic field, μ_0 the free space permeability, and ϵ_0 the free space permittivity. From (1) and (2), the vector wave equation for $\mathbf{E}$ becomes

$$\nabla \times \nabla \times \mathbf{E} - k_0^2\epsilon\mathbf{E} = 0, \tag{3}$$

with $k_0 = \omega\sqrt{\mu_0\epsilon_0}$. Let

$$\epsilon(\mathbf{r}) = \epsilon_b(\mathbf{r}) + \epsilon_s(\mathbf{r}), \tag{4}$$

where $\epsilon_b(\mathbf{r})$ is the spatially dependent background dielectric constant that describes the random medium without the moving object(s) of interest and $\epsilon_s(\mathbf{r})$ is the contrast due to the moving scattering object to be imaged, as shown in Fig. 2. Therefore, with use of (4), (3) becomes

$$\nabla \times \nabla \times \mathbf{E} - k_0^2\epsilon_b\mathbf{E} = k_0^2\epsilon_s\mathbf{E}. \tag{5}$$

Recognizing that $\nabla \times \nabla \times \mathbf{E}_b - k_0^2\epsilon_b\mathbf{E}_b = 0$, (5) can be written as

$$\nabla \times \nabla \times \mathbf{E}_s - k_0^2\epsilon_b\mathbf{E}_s = k_0^2\epsilon_s\mathbf{E}. \tag{6}$$

The Green's function wave equation corresponding to (6) is

$$\nabla \times \nabla \times \mathbf{G}_\mathbf{p}(\mathbf{r}, \mathbf{r}') - k_0^2\epsilon_b(\mathbf{r})\mathbf{G}_\mathbf{p}(\mathbf{r}, \mathbf{r}') = -\delta(\mathbf{r} - \mathbf{r}')\hat{\mathbf{p}}, \tag{7}$$

where the position vectors are now included for clarity, $\mathbf{r}'$ is the (equivalent) source location and $\hat{\mathbf{p}}$ is drawn from the set of orthogonal unit vectors to produce the tensor $\mathbf{G}$. Using (7)

and superposition to write the integral equation corresponding to (6), and with $\mathbf{E} = \mathbf{E}_b + \mathbf{E}_s$, we have

$$\mathbf{E}(\mathbf{r}) = \mathbf{E}_b(\mathbf{r}) - \int k_0^2 \epsilon_s(\mathbf{r}') \mathbf{G}(\mathbf{r}, \mathbf{r}') \mathbf{E}(\mathbf{r}') d\mathbf{r}' \tag{8}$$

as the exact representation for the scattering problem. The use of a tensor Green's function in (8) provides for multiple scattering from the random background medium, including related depolarization and polarization coupling, in forming the integral representation of the vector scattered electric field. Implicit in the ensuing development is the dependence of measurable intensities on the incident field, and assuming a laser excitation, on the specifics of the illumination.

The predominant underlying theory in statistical optics deals with Gaussian fields [1]. In the relevant experiments, this implies both adequate temporal coherence and the detection of a single polarization state [31, 32]. This is achieved by making (intensity) measurements through a polarizer. Consequently, the $\hat{\mathbf{d}}$ component of the electric field is sifted (describing a specific polarization state), so (8) assumes the scalar form

$$\begin{aligned} E(\mathbf{r}) &= E_b(\mathbf{r}) + \int O(\mathbf{r}') \; \hat{\mathbf{d}} \cdot [\mathbf{G}(\mathbf{r}, \mathbf{r}') \mathbf{E}(\mathbf{r}')] \, d\mathbf{r}' \\ &= E_b(\mathbf{r}) + E_s(\mathbf{r}). \end{aligned} \tag{9}$$

Without loss of generality, we can define a simplified scalar object function as

$$O(\mathbf{r}') = -k_0^2 \epsilon_s(\mathbf{r}'). \tag{10}$$

The development of the imaging formulation exploits this simplified scalar picture with the exact interpretation that the vector field is being sampled at the detector through a polarizer.

III. DETECTED FIELD MOMENTS

Consider a point detector located at $\mathbf{r} = \mathbf{r}_d$, as in Fig. 1, and define the field at this point by $E(\mathbf{r}_d) \equiv E_d$, where the spatial argument is represented as a subscript for compactness. We assume measurements that reflect E_d at a sequence of object positions defined by a reference position $\mathbf{r}_0$ and a translation vector $\Delta\mathbf{r}$. We can thus describe the field at the detector as $E_d(\mathbf{r}_0)$ with the object at some reference position and $E_d(\mathbf{r}_0 + \Delta\mathbf{r})$ with the object at the displaced position defined by $\Delta\mathbf{r}$.

The background scattering process is treated as random, and the fields at some $\mathbf{r}_d$ can be considered as a random phasor sum with developed statistics so that E_d is zero-mean circular Gaussian [1]. This also provides access to a moment theorem made widely known by Reed [7], and with stationary statistics the special cases of the second and fourth moments are related in a manner presented earlier by Siegert [34]. We define the statistical average $\langle\cdot\rangle$ as being over background scatterer configuration. Section VIII considers the practical aspects of how the average is determined experimentally with speckle intensity data obtained by a camera.

The intensity is assumed to be measured, and we write the intensity at the detector as $I_d = |E_d|^2$, where a normalized impedance is assumed. The fourth order field moment provides the measured intensity correlation over object position as [7]

$$\begin{aligned}\langle I_d(\mathbf{r}_0)I_d(\mathbf{r}_0+\Delta\mathbf{r})\rangle &= \langle E_d(\mathbf{r}_0)E_d^*(\mathbf{r}_0)E_d(\mathbf{r}_0+\Delta\mathbf{r})E_d^*(\mathbf{r}_0+\Delta\mathbf{r})\rangle \\ &= \langle I_d(\mathbf{r}_0)\rangle\langle I_d(\mathbf{r}_0+\Delta\mathbf{r})\rangle + \langle E_d^*(\mathbf{r}_0)E_d(\mathbf{r}_0+\Delta\mathbf{r})\rangle\langle E_d^*(\mathbf{r}_0+\Delta\mathbf{r})E_d(\mathbf{r}_0)\rangle \\ &= \langle I_d(\mathbf{r}_0)\rangle\langle I_d(\mathbf{r}_0+\Delta\mathbf{r})\rangle + |\langle E_d^*(\mathbf{r}_0)E_d(\mathbf{r}_0+\Delta\mathbf{r})\rangle|^2 . \qquad (11)\end{aligned}$$

Equation (11) will be used throughout our development.

It is convenient to define a normalized field

$$\tilde{E} = \frac{E}{\langle I\rangle^{1/2}}, \qquad (12)$$

with $I = |E|^2$, and a normalized intensity

$$\tilde{I} = \frac{(I - \langle I\rangle)}{\langle I\rangle}. \qquad (13)$$

The normalization for field (giving $\tilde{E}$) in (12) is consistent with that for intensity ($\tilde{I}$) in (13). For a Gaussian field [7], $\langle I^2\rangle = 2\langle I\rangle^2$, so the intensity variance is

$$\begin{aligned}\sigma_I^2 &= \langle I^2\rangle - \langle I\rangle^2 \\ &= \langle I\rangle^2. \qquad (14)\end{aligned}$$

The contrast ratio is thus $\sigma_I/\langle I\rangle = 1$ [1].

The second order field correlation over object position, measured at the detector, is

$$G^{(1)}(\mathbf{r}_d;\mathbf{r}_0,\mathbf{r}_0+\Delta\mathbf{r}) = \langle E_d^*(\mathbf{r}_0)E_d(\mathbf{r}_0+\Delta\mathbf{r})\rangle \equiv G^{(1)}(\mathbf{r}_0,\mathbf{r}_0+\Delta\mathbf{r}), \qquad (15)$$

where we use a common notation for the second order field moment ($G^{(1)}(\cdot)$) and a compact argument to simplify the form of subsequent expressions, where the implication is a

measurement at a single detector point ($\mathbf{r}_d$). With the use of normalizations involving the mean intensity, $\langle \tilde{E}_d^*(\mathbf{r})\tilde{E}_d(\mathbf{r}+\Delta\mathbf{r})\rangle \rightarrow \langle \tilde{E}_d^*(0)\tilde{E}_d(\Delta\mathbf{r})\rangle$, and the normalized field (and intensity) correlations become independent of the object reference position $\mathbf{r}$. The normalized averaged field correlation measured at the detector point as the object is scanned is then

$$\begin{aligned} g^{(1)}(\Delta\mathbf{r}) &= \langle \tilde{E}_d^*(0)\tilde{E}_d(\Delta\mathbf{r})\rangle \\ &= \frac{G^{(1)}(\mathbf{r}_0, \mathbf{r}_0+\Delta\mathbf{r})}{\langle I_d(\mathbf{r}_0)\rangle^{1/2}\langle I_d(\mathbf{r}_0+\Delta\mathbf{r})\rangle^{1/2}}. \end{aligned} \tag{16}$$

Use of (12) or (13) and (16) with (11) gives

$$\begin{aligned} \langle \tilde{I}_d(\mathbf{r}_0)\tilde{I}_d(\mathbf{r}_0+\Delta\mathbf{r})\rangle &= \langle \tilde{I}_d(0)\tilde{I}_d(\Delta\mathbf{r})\rangle \\ &= \left|g^{(1)}(\Delta\mathbf{r})\right|^2. \end{aligned} \tag{17}$$

While object information is in principle embedded in (17), this interpretation of normalized measured data does not provide for imaging. We present a theory that provides a clear path to a method to invert measured data and form an image.

IV. RELATIONSHIP BETWEEN OBJECT AND DETECTED FIELD MOMENTS

Returning to (9), we write the field at the detector as a superposition of that due to the background random scatter (E_{db}) and that due to the object (defined as the scattered field, E_{ds}). Expanding the second-order field correlation with this field superposition, we have

$$\begin{aligned} \langle E_d^*(\mathbf{r}_0)E_d(\mathbf{r}_0+\Delta\mathbf{r})\rangle &= \langle E_{db}^*(\mathbf{r}_0)E_{db}(\mathbf{r}_0+\Delta\mathbf{r})\rangle + \langle E_{db}^*(\mathbf{r}_0)E_{ds}(\mathbf{r}_0+\Delta\mathbf{r})\rangle \\ &\quad + \langle E_{ds}^*(\mathbf{r}_0)E_{db}(\mathbf{r}_0+\Delta\mathbf{r})\rangle + \langle E_{ds}^*(\mathbf{r}_0)E_{ds}(\mathbf{r}_0+\Delta\mathbf{r})\rangle \\ &= \langle I_{db}\rangle + \langle E_{db}^*E_{ds}(\mathbf{r}_0+\Delta\mathbf{r})\rangle + \langle E_{ds}^*(\mathbf{r}_0)E_{db}\rangle \\ &\quad + \langle E_{ds}^*(\mathbf{r}_0)E_{ds}(\mathbf{r}_0+\Delta\mathbf{r})\rangle. \end{aligned} \tag{18}$$

Note that $E_{db}(\mathbf{r}_0) = E_{db}(\mathbf{r}_0+\Delta\mathbf{r}) = E_{db}$, because the background field is that without the object (the incident field), so $\langle E_{db}^*(\mathbf{r}_0)E_{db}(\mathbf{r}_0+\Delta\mathbf{r})\rangle = \langle E_{db}^*E_{db}\rangle = \langle I_{db}\rangle$, dictated by the optical excitation, the scattering medium, and the detector location, but independent of the moving object.

In (18), referring to (9) and (10), $E_{ds} = E_s(\mathbf{r}_d)$, so with the object at the reference position $\mathbf{r}_0$,

$$E_{ds}(\mathbf{r}_0) = \int O(\mathbf{r}';\mathbf{r}_0)\ \hat{\mathbf{d}}\cdot[\mathbf{G}(\mathbf{r}_d,\mathbf{r}')\mathbf{E}(\mathbf{r}')]\,d\mathbf{r}', \tag{19}$$

where $O(\mathbf{r}')$ defines the object through (10). This allows us to build expressions for each of the three remaining terms in (18).

First, from (19) and with a shift in object position of $\Delta\mathbf{r}$,

$$\begin{aligned}\langle E^*_{ds}(\mathbf{r}_0)E_{ds}(\mathbf{r}_0+\Delta\mathbf{r})\rangle &= \langle \int O^*(\mathbf{r}';\mathbf{r}_0)\hat{\mathbf{d}}\cdot[\mathbf{G}(\mathbf{r}_d,\mathbf{r}')\mathbf{E}(\mathbf{r}')]^*\,d\mathbf{r}' \\ &\qquad \int O(\mathbf{r}';\mathbf{r}_0+\Delta\mathbf{r})\ \hat{\mathbf{d}}\cdot[\mathbf{G}(\mathbf{r}_d,\mathbf{r}')\mathbf{E}(\mathbf{r}')]\,d\mathbf{r}'\rangle \\ &= \langle \int d\mathbf{r}' \int d\mathbf{r}'' O^*(\mathbf{r}';\mathbf{r}_0)\ \hat{\mathbf{d}}\cdot[\mathbf{G}(\mathbf{r}_d,\mathbf{r}')\mathbf{E}(\mathbf{r}')]^* \\ &\qquad O(\mathbf{r}'';\mathbf{r}_0+\Delta\mathbf{r})\hat{\mathbf{d}}\cdot[\mathbf{G}(\mathbf{r}_d,\mathbf{r}'')\mathbf{E}(\mathbf{r}'')]\rangle \\ &= G^{(1)}_{ss}(\mathbf{r}_0,\mathbf{r}_0+\Delta\mathbf{r}) \\ &= \langle I_{ds}(\mathbf{r}_0)\rangle^{1/2}\langle I_{ds}(\mathbf{r}_0+\Delta\mathbf{r})\rangle^{1/2} g^{(1)}_{ss}(\Delta\mathbf{r}), \end{aligned} \tag{20}$$

so

$$\begin{aligned} g^{(1)}_{ss}(\Delta\mathbf{r}) &= \langle I_{ds}(\mathbf{r}_0)\rangle^{-1/2}\langle I_{ds}(\mathbf{r}_0+\Delta\mathbf{r})\rangle^{-1/2} \\ &\qquad \langle \int d\mathbf{r}' \int d\mathbf{r}'' O^*(\mathbf{r}';\mathbf{r}_0)\ \hat{\mathbf{d}}\cdot[\mathbf{G}(\mathbf{r}_d,\mathbf{r}')\mathbf{E}(\mathbf{r}')]^* O(\mathbf{r}'';\mathbf{r}_0+\Delta\mathbf{r})\hat{\mathbf{d}}\cdot[\mathbf{G}(\mathbf{r}_d,\mathbf{r}'')\mathbf{E}(\mathbf{r}'')]\rangle \\ &= \langle \tilde{E}^*_{ds}(0)\tilde{E}_{ds}(\Delta\mathbf{r})\rangle \\ &= a_{ss}(\Delta\mathbf{r})e^{i\phi_{ss}(\Delta\mathbf{r})}. \end{aligned} \tag{21}$$

We note from (21) that the normalization results in $|g^{(1)}_{ss}(0)| = 1$, so that $a_{ss}(0) = 1$ and $\phi_{ss}(0) = 0$. Notice that $g^{(1)}_{ss}$ in principle provides access to a measure of the spatial correlation of the object, something we pursue later. The challenge is to relate $g^{(1)}_{ss}$ to a measurable quantity, because I_{ds} is not directly available.

Like (20), using (19), we have

$$\begin{aligned}\langle E^*_{db}(\mathbf{r}_0)E_{ds}(\mathbf{r}_0+\Delta\mathbf{r})\rangle &= \langle E^*_{db}\int O(\mathbf{r}';\mathbf{r}_0+\Delta\mathbf{r})\hat{\mathbf{d}}\cdot[\mathbf{G}(\mathbf{r}_d,\mathbf{r}')\mathbf{E}(\mathbf{r}')]\,d\mathbf{r}'\rangle \\ &= \langle I_{db}\rangle^{1/2}\langle I_{ds}(\mathbf{r}_0+\Delta\mathbf{r})\rangle^{1/2} g^{(1)}_{bs}(\Delta\mathbf{r}). \end{aligned} \tag{22}$$

Hence,

$$\begin{aligned} g^{(1)}_{bs}(\Delta\mathbf{r}) &= \langle \tilde{E}^*_{db}\tilde{E}_{ds}(\Delta\mathbf{r})\rangle \\ &= a_{bs}(\Delta\mathbf{r})e^{i\phi_{bs}(\Delta\mathbf{r})}, \end{aligned} \tag{23}$$

and $|g^{(1)}_{bs}(0)| = 0$.

The final term in (18) is thus

$$\begin{aligned}\langle E^*_{ds}(\mathbf{r}_0)E_{db}\rangle &= \langle I_{ds}(\mathbf{r}_0)\rangle^{1/2}\langle I_{db}\rangle^{1/2}g^{(1)}_{sb}(0)\\ &\equiv \langle I_{ds}(\mathbf{r}_0)\rangle^{1/2}\langle I_{db}\rangle^{1/2}g^{(1)*}_{bs}(0),\end{aligned} \tag{24}$$

where we have

$$\begin{aligned}g^{(1)}_{sb}(0) &= \langle \tilde{E}^*_{ds}(\mathbf{r})\tilde{E}_{db}\rangle\\ &= a_{sb}(0)e^{i\phi_{sb}(0)}\\ &= e^{i\phi_{sb}(0)}\\ &= e^{-i\phi_{bs}(0)}\\ &\equiv g^{(1)*}_{bs}(0).\end{aligned} \tag{25}$$

Collecting the various terms, we can thus write the field correlation over object position measured at the detector point, from (18), as

$$\begin{aligned}\langle E^*_d(\mathbf{r}_0)E_d(\mathbf{r}_0+\Delta\mathbf{r})\rangle &= \langle E^*_{db}E_{db}\rangle + \langle E^*_{db}(\mathbf{r}_0)E_{ds}(\mathbf{r}_0+\Delta\mathbf{r})\rangle\\ &\quad + \langle E^*_{ds}(\mathbf{r}_0)E_{db}(\mathbf{r}_0+\Delta\mathbf{r})\rangle + \langle E^*_{ds}(\mathbf{r}_0)E_{ds}(\mathbf{r}_0+\Delta\mathbf{r})\rangle\\ &= \langle I_{db}\rangle + \langle I_{db}\rangle^{1/2}\langle I_{ds}(\mathbf{r}_0+\Delta\mathbf{r})\rangle^{1/2}g^{(1)}_{bs}(\Delta\mathbf{r})\\ &\quad + \langle I_{ds}(\mathbf{r}_0)\rangle^{1/2}\langle I_{db}\rangle^{1/2}g^{(1)*}_{bs}(0)\\ &\quad + \langle I_{ds}(\mathbf{r}_0)\rangle^{1/2}\langle I_{ds}(\mathbf{r}_0+\Delta\mathbf{r})\rangle^{1/2}g^{(1)}_{ss}(\Delta\mathbf{r}).\end{aligned} \tag{26}$$

Interpretations of (26) will prove useful in imaging based on motion in scattering media.

V. PHYSICAL BASIS OF $g^{(1)}_{ss}(\Delta\mathbf{r})$ AND $g^{(1)}_{bs}(\Delta\mathbf{r})$

Experimental evidence indicates that a macroscopic moving object's geometrical parameters can be determined from an average speckle intensity correlation over translated object position [32, 33]. In the special case of an aperture function, total decorrelation occurs at a distance corresponding to the aperture width [32]. From (26), this information about the object is described by $|g^{(1)}_{ss}(\Delta\mathbf{r})|$. From (21) and considering the case of an aperture, this implies that the scattered field from the object and its translated version survive an averaging process. This availability of field information despite the intervening heavily scattering random medium is consistent with experiments that showed that the incident field on a

random medium can be determined from transmitted speckle intensity correlations over the scanned field position [31]. Generalizing to results from an experiment with an absorbing patch [33], the patch diameter was available from a dip in the speckle correlation. This line of evidence suggests that the normalized scattered field associated with the moving object, represented in the field correlation of (26), is retained through an averaging process involving reconfiguration of the background randomly located scatterers. Macroscopically, referring to Fig. 1, this situation occurs when the object and the translated object share a joint spatial support, and follows from the concept of correlated incident fields when imaging based on field translation over the remote side of a randomly scattering medium [31]. We therefore arrive at the conclusion that $g_{ss}^{(1)}(\Delta\mathbf{r})$ has correlated scattered field contributions from the object and the shifted object when they share a common spatial support. We will separate $g_{ss}^{(1)}(\Delta\mathbf{r})$ into short-range and long-range terms, as shown in Fig. 3. The short range decorrelation has been shown to be sensitive to the microstructure and subwavelength features and the long range to macroscopic object information through a joint spatial support picture [32]. We will separately address the role of $g_{bs}^{(1)}$.

The autocorrelation of the object function is

$$\Gamma(\Delta\mathbf{r}) = \int d\mathbf{r}' O^*(\mathbf{r}')O(\mathbf{r}' + \Delta\mathbf{r}). \tag{27}$$

A comparison of (21) and (27), under conditions of sufficient random scatter for developed statistics, suggests

$$\begin{aligned} g_{ss}^{(1)}(\Delta\mathbf{r}) &= \gamma(\Delta\mathbf{r}) \\ &= \int d\mathbf{r}' \tilde{O}^*(\mathbf{r}')\tilde{O}(\mathbf{r}' + \Delta\mathbf{r}), \end{aligned} \tag{28}$$

where γ is the normalized autocorrelation and $\tilde{O}$ is the normalized object function. With (28), information related to $g_{ss}^{(1)}(\Delta\mathbf{r})$ leads to a means to retrieve $\tilde{O}$, as we will describe.

Possibly less obvious is the role of $g_{bs}^{(1)}(\Delta\mathbf{r})$ and its character, upon observation of the average field correlation in (22). It is insightful to consider the *Gedankenexperiment* of a detected field correlation without displacement. Based on (18), the mean intensity at the detector point with the object at the reference position is

$$\begin{aligned} \langle I_d(\mathbf{r}_0)\rangle &= \langle E_d^*(\mathbf{r}_0)E_d(\mathbf{r}_0)\rangle \\ &= \langle I_{db}\rangle + 2\Re\{\langle E_{db}^* E_{ds}(\mathbf{r}_0)\rangle\} + \langle I_{ds}(\mathbf{r}_0)\rangle \\ &= \langle I_{db}\rangle + \langle I_{ds}(\mathbf{r}_0)\rangle + \langle I_{db}\rangle^{1/2}\langle I_{ds}(\mathbf{r}_0)\rangle^{1/2} 2\Re\{g_{bs}^{(1)}(0)\}, \end{aligned} \tag{29}$$

with $\Re\{\cdot\}$ the real part. The only way to describe a decrease in mean intensity with the introduction of an object is by $g_{bs}^{(1)}(0)$. Therefore, in general, $g_{bs}^{(1)}$ must be retained in the intensity correlation expressions. Also, clear from (29), $g_{bs}^{(1)}(0)$ has negative real part for situations where $\langle I_{db}\rangle > \langle I_d\rangle$. From (23), one might anticipate that $g_{bs}^{(1)}(\Delta\mathbf{r})$ will reduce to zero when the object translation is large compared to λ. This position rests on substantial uncorrelated scatter associated with the moving object in relation to the background random scattering medium. Note from (22) that $g_{bs}^{(1)}$ is normalized by $\langle I_{ds}\rangle$, which provides the scattering strength. If $\langle I_{ds}\rangle^{1/2} g_{bs}^{(1)}(\Delta\mathbf{r})$ were available, this could provide object information.

By analogy with field correlations over frequency [35], a random phasor sum description in the Gaussian field limit indicates a pathlength distribution with a differential phase shift $k|\Delta\mathbf{r}| < \lambda$, suggesting a decorrelation over $|\Delta\mathbf{r}| \sim \lambda$. Irrespective of the details of the moving object, we therefore expect a contribution from point scatterer motion on this length scale, and that this will influence both $g_{ss}^{(1)}$ and $g_{bs}^{(1)}$. Embedded in this will be nanostructure information about the object.

VI. DETECTOR INTENSITY CORRELATION

From (11), the intensity correlation at the detector point, measured over object position, is

$$\langle I_d(\mathbf{r}) I_d(\mathbf{r}+\Delta\mathbf{r})\rangle = \langle I_d(\mathbf{r})\rangle\langle I_d(\mathbf{r}+\Delta\mathbf{r})\rangle + |\langle E_d^*(\mathbf{r}) E_d(\mathbf{r}+\Delta\mathbf{r})\rangle|^2 . \tag{30}$$

Using (26) and arranging into terms involving orders of $g_{ss}^{(1)}$,

$$\begin{aligned}
|\langle E_d^*(\mathbf{r}) E_d(\mathbf{r}+\Delta\mathbf{r})\rangle|^2 = \Big\{ & \langle I_{db}\rangle^2 \\
& + \langle I_{db}\rangle^{3/2} \left[\langle I_{ds}(\mathbf{r}+\Delta\mathbf{r})\rangle^{1/2} 2\Re\{g_{bs}^{(1)}(\Delta\mathbf{r})\} + \langle I_{ds}(\mathbf{r})\rangle^{1/2} 2\Re\{g_{bs}^{(1)}(0)\} \right] \\
& + \langle I_{db}\rangle \langle I_{ds}(\mathbf{r})\rangle^{1/2} \langle I_{ds}(\mathbf{r}+\Delta\mathbf{r})\rangle^{1/2} 2\Re\{g_{bs}^{(1)}(0) g_{bs}^{(1)}(\Delta\mathbf{r})\} \\
& + \langle I_{db}\rangle \langle I_{ds}(\mathbf{r})\rangle |g_{bs}^{(1)}(0)|^2 + \langle I_{db}\rangle \langle I_{ds}(\mathbf{r}+\Delta\mathbf{r})\rangle |g_{bs}^{(1)}(\Delta\mathbf{r})|^2 \Big\} \\
& + \Big\{ \langle I_{db}\rangle^{1/2} \Big[\langle I_{ds}(\mathbf{r})\rangle^{1/2} \langle I_{ds}(\mathbf{r}+\Delta\mathbf{r})\rangle 2\Re\{g_{bs}^{(1)}(\Delta\mathbf{r}) g_{ss}^{(1)*}(\Delta\mathbf{r})\} \\
& \qquad + \langle I_{ds}(\mathbf{r})\rangle \langle I_{ds}(\mathbf{r}+\Delta\mathbf{r})\rangle^{1/2} 2\Re\{g_{bs}^{(1)}(0) g_{ss}^{(1)}(\Delta\mathbf{r})\} \Big] \\
& + \langle I_{db}\rangle \langle I_{ds}(\mathbf{r})\rangle^{1/2} \langle I_{ds}(\mathbf{r}+\Delta\mathbf{r})\rangle^{1/2} 2\Re\{g_{ss}^{(1)}(\Delta\mathbf{r})\} \Big\} \\
& + \langle I_{ds}(\mathbf{r})\rangle \langle I_{ds}(\mathbf{r}+\Delta\mathbf{r})\rangle |g_{ss}^{(1)}(\Delta\mathbf{r})|^2 .
\end{aligned} \tag{31}$$

It is convenient to convert raw measured speckle intensity data into normalized form ($\tilde{I}$) using (13). This step also simplifies the mathematical representation. In normalized form, (30) becomes

$$\langle \tilde{I}_d(\mathbf{r}_0)\tilde{I}_d(\mathbf{r}_0+\Delta\mathbf{r})\rangle = \left|\langle \tilde{E}_d^*(\mathbf{r}_0)\tilde{E}_d(\mathbf{r}_0+\Delta\mathbf{r})\rangle\right|^2, \tag{32}$$

where

$$\tilde{E}_d(\mathbf{r}_0) = \frac{E_d(\mathbf{r}_0)}{\langle I_d(\mathbf{r}_0)\rangle^{1/2}} \tag{33}$$

$$\tilde{E}_d(\mathbf{r}_0+\Delta\mathbf{r}) = \frac{E_d(\mathbf{r}_0+\Delta\mathbf{r})}{\langle I_d(\mathbf{r}_0+\Delta\mathbf{r})\rangle^{1/2}}, \tag{34}$$

and, as before, the normalized fields depend only on the translation, $\Delta\mathbf{r}$. Drawing on (31) - (34), we can write

$$\begin{aligned}\langle \tilde{I}_d(\mathbf{r}_0)\tilde{I}_d(\mathbf{r}_0+\Delta\mathbf{r})\rangle = {} & C_0(\Delta\mathbf{r};\mathbf{r}_0) \\ & + C_{11}(\Delta\mathbf{r};\mathbf{r}_0)2\Re\{g_{bs}^{(1)}(\Delta\mathbf{r})g_{ss}^{(1)*}(\Delta\mathbf{r})\} + C_{12}(\Delta\mathbf{r};\mathbf{r}_0)2\Re\{g_{bs}^{(1)}(0)g_{ss}^{(1)}(\Delta\mathbf{r})\} \\ & + C_{13}(\Delta\mathbf{r};\mathbf{r}_0)2\Re\{g_{ss}^{(1)}(\Delta\mathbf{r})\} + C_2(\Delta\mathbf{r};\mathbf{r}_0)|g_{ss}^{(1)}(\Delta\mathbf{r})|^2,\end{aligned} \tag{35}$$

where, referring to (31),

$$\begin{aligned} C_0(\Delta\mathbf{r};\mathbf{r}_0) = {} & \langle I_d(\mathbf{r}_0)\rangle^{-1}\langle I_d(\mathbf{r}_0+\Delta\mathbf{r})\rangle^{-1}\Big\{\langle I_{db}\rangle^2 \\ & + \langle I_{db}\rangle^{3/2}\left[\langle I_{ds}(\mathbf{r}_0+\Delta\mathbf{r})\rangle^{1/2}2\Re\{g_{bs}^{(1)}(\Delta\mathbf{r})\} + \langle I_{ds}(\mathbf{r}_0)\rangle^{1/2}2\Re\{g_{bs}^{(1)}(0)\}\right] \\ & + \langle I_{db}\rangle\langle I_{ds}(\mathbf{r}_0)\rangle^{1/2}\langle I_{ds}(\mathbf{r}_0+\Delta\mathbf{r})\rangle^{1/2}2\Re\{g_{bs}^{(1)}(0)g_{bs}^{(1)}(\Delta\mathbf{r})\} \\ & + \langle I_{db}\rangle\langle I_{ds}(\mathbf{r}_0)\rangle + \langle I_{db}\rangle\langle I_{ds}(\mathbf{r}_0+\Delta\mathbf{r})\rangle|g_{bs}^{(1)}(\Delta\mathbf{r})|^2\Big\} \\ C_{11}(\Delta\mathbf{r};\mathbf{r}_0) = {} & \langle I_d(\mathbf{r}_0)\rangle^{-1}\langle I_d(\mathbf{r}_0+\Delta\mathbf{r})\rangle^{-1}\langle I_{db}\rangle^{1/2}\langle I_{ds}(\mathbf{r}_0)\rangle^{1/2}\langle I_{ds}(\mathbf{r}_0+\Delta\mathbf{r})\rangle \\ C_{12}(\Delta\mathbf{r};\mathbf{r}_0) = {} & \langle I_d(\mathbf{r}_0)\rangle^{-1}\langle I_d(\mathbf{r}_0+\Delta\mathbf{r})\rangle^{-1}\langle I_{db}\rangle^{1/2}\langle I_{ds}(\mathbf{r}_0)\rangle\langle I_{ds}(\mathbf{r}_0+\Delta\mathbf{r})\rangle^{1/2} \\ C_{13}(\Delta\mathbf{r};\mathbf{r}_0) = {} & \langle I_d(\mathbf{r}_0)\rangle^{-1}\langle I_d(\mathbf{r}_0+\Delta\mathbf{r})\rangle^{-1}\langle I_{db}\rangle\langle I_{ds}(\mathbf{r}_0)\rangle^{1/2}\langle I_{ds}(\mathbf{r}_0+\Delta\mathbf{r})\rangle^{1/2} \\ C_2(\Delta\mathbf{r};\mathbf{r}_0) = {} & \langle I_d(\mathbf{r}_0)\rangle^{-1}\langle I_d(\mathbf{r}_0+\Delta\mathbf{r})\rangle^{-1}\langle I_{ds}(\mathbf{r}_0)\rangle\langle I_{ds}(\mathbf{r}_0+\Delta\mathbf{r})\rangle. \end{aligned} \tag{36}$$

The normalizations and spatial dependencies in (35) and (36) warrant special note. In (35), $\langle \tilde{I}_d(\mathbf{r}_0)\tilde{I}_d(\mathbf{r}_0+\Delta\mathbf{r})\rangle$ uses $\langle I_d(\mathbf{r}_0)\rangle$ and $\langle I_d(\mathbf{r}_0+\Delta\mathbf{r})\rangle$ for scaling, according to (13). This results in $\langle \tilde{I}_d(\mathbf{r}_0)^2\rangle = 1$, independent of $\mathbf{r}_0$. However, the features in this correlation as $\Delta\mathbf{r}$ is varied can depend on $\mathbf{r}_0$, hence the inclusion of this dependency on the left of (35). The normalizations used for $g_{bs}^{(1)}(\Delta\mathbf{r})$ and $g_{ss}^{(1)}(\Delta\mathbf{r})$ that make them independent of $\mathbf{r}_0$ are different to those used in forming $\tilde{I}_d$. Consequently, there are products and ratios of various mean

intensity forms in (36) that depend on $\mathbf{r}_0$. The $\mathbf{r}_0$ dependency on the right-hand side of (35) is therefore incorporated into the coefficient functions in (36) and through the various mean terms. In special arrangements, the coefficients in (35) can be written (or approximated) as being independent of $\mathbf{r}_0$ (and $\Delta\mathbf{r}$).

We can sift $g_{ss}^{(1)}$ from (35), with use of (36), by separating the real ($\Re$) and imaginary ($\Im$) parts of the field correlations associated with C_{1j} as

$$\begin{aligned}\langle \tilde{I}_d(\mathbf{r}_0)\tilde{I}_d(\mathbf{r}_0+\Delta\mathbf{r})\rangle &= C_0(\Delta\mathbf{r};\mathbf{r}_0)\\ &+2\left[C_{11}(\Delta\mathbf{r};\mathbf{r}_0)\Re\{g_{bs}^{(1)}(\Delta\mathbf{r})\}+C_{12}(\Delta\mathbf{r};\mathbf{r}_0)\Re\{g_{bs}^{(1)}(0)\}+C_{13}(\Delta\mathbf{r};\mathbf{r}_0)\right]\Re\{g_{ss}^{(1)}(\Delta\mathbf{r})\}\\ &+2\left[C_{11}(\Delta\mathbf{r};\mathbf{r}_0)\Im\{g_{bs}^{(1)}(\Delta\mathbf{r})\}-C_{12}(\Delta\mathbf{r};\mathbf{r}_0)\Im\{g_{bs}^{(1)}(0)\}\right]\Im\{g_{ss}^{(1)}(\Delta\mathbf{r})\}\\ &+C_2(\Delta\mathbf{r};\mathbf{r}_0)|g_{ss}^{(1)}(\Delta\mathbf{r})|^2\\ &\equiv C_0(\Delta\mathbf{r};\mathbf{r}_0)+2C_{1r}(\Delta\mathbf{r};\mathbf{r}_0)\Re\{g_{ss}^{(1)}(\Delta\mathbf{r})\}+2C_{1i}(\Delta\mathbf{r};\mathbf{r}_0)\Im\{g_{ss}^{(1)}(\Delta\mathbf{r})\}\\ &+C_2(\Delta\mathbf{r};\mathbf{r}_0)|g_{ss}^{(1)}(\Delta\mathbf{r})|^2, \end{aligned} \tag{37}$$

where the C coefficients in general vary with $\Delta\mathbf{r}$ and $\mathbf{r}_0$ and

$$\begin{aligned}C_{1r}(\Delta\mathbf{r};\mathbf{r}_0)&=\Re\{C_1(\Delta\mathbf{r};\mathbf{r}_0)\}=C_{11}(\Delta\mathbf{r};\mathbf{r}_0)\Re\{g_{bs}^{(1)}(\Delta\mathbf{r})\}+C_{12}(\Delta\mathbf{r};\mathbf{r}_0)\Re\{g_{bs}^{(1)}(0)\}+C_{13}(\Delta\mathbf{r};\mathbf{r}_0)\\ C_{1i}(\Delta\mathbf{r};\mathbf{r}_0)&=\Im\{C_1(\Delta\mathbf{r};\mathbf{r}_0)\}=C_{11}(\Delta\mathbf{r};\mathbf{r}_0)\Im\{g_{bs}^{(1)}(\Delta\mathbf{r})\}-C_{12}(\Delta\mathbf{r};\mathbf{r}_0)\Im\{g_{bs}^{(1)}(0)\}.\end{aligned} \tag{38}$$

Equation (37) can thus be written as

$$\boxed{\langle \tilde{I}_d(\mathbf{r}_0)\tilde{I}_d(\mathbf{r}_0+\Delta\mathbf{r})\rangle = C_0(\Delta\mathbf{r};\mathbf{r}_0)+2\Re\left\{C_1^*(\Delta\mathbf{r};\mathbf{r}_0)g_{ss}^{(1)}(\Delta\mathbf{r})\right\}+C_2(\Delta\mathbf{r};\mathbf{r}_0)|g_{ss}^{(1)}(\Delta\mathbf{r})|^2.} \tag{39}$$

Equation (39) is our key result, and this will be used to consider various object and scatter regimes. The arrangement is in terms of orders of $g_{ss}^{(1)}$, the complex normalized field correlation in (21) that we have written in terms of the object autocorrelation function (28). Figure 3 shows the character expected for $g_{ss}^{(1)}$ based on earlier experiments [32]. The coefficients C_0, C_1 and C_2 depend on the relative position of the object and allow for non-stationary statistics through position-dependent means. With sufficient scatter it may suffice to treat these as constants [33]. Both C_0 and C_1 are non-zero only when there is a background field at the detector, defined as the field without the moving object. With an aperture in an opaque screen, absence of the object corresponds to a closed aperture and hence there is no background field at the detector, resulting in a contribution from only the third term in (39). Contained within C_0 and C_1 are correlations between the background

field and the field scattered by the object, $g_{bs}^{(1)}$. Our experiments with absorbing patches [33] indicate that C_1/C_0 is small and possibly negligible, that it diminishes with increasing levels of background scatter, and that it increases with reducing object scatter ($\langle I_{ds} \rangle$). With non-zero C_0, the ratio C_2/C_0 decreases with an increase in background scatter. These coefficients thus become a measure of the character of the background scattering medium in which the object is moving. While (39) is a compact expression relating measured intensity correlations to $g_{ss}^{(1)}$ and hence the object through (28), I_{ds} and $g_{bs}^{(1)}$ are not directly obtained from any measurement. Therefore, a tractable path to imaging requires approximations or assumptions to access the object function, O.

VII. CORRELATION LENGTH SCALES, OBJECT SCATTERING REGIMES AND EXPERIMENTAL EVIDENCE

There are two important field correlations in (39) that carry information about the moving object, $g_{bs}^{(1)}(\Delta\mathbf{r})$ (that appears in $C_0(\Delta\mathbf{r};\mathbf{r}_0)$ and $C_1(\Delta\mathbf{r};\mathbf{r}_0) = C_{1r}(\Delta\mathbf{r};\mathbf{r}_0) + iC_{1i}(\Delta\mathbf{r};\mathbf{r}_0)$) and $g_{ss}^{(1)}(\Delta\mathbf{r})$ (see Fig. 3). At this point, we expect $g_{bs}^{(1)}(\Delta\mathbf{r})$ to reduce from unit magnitude to zero as $\Delta\mathbf{r}$ increases from zero to the length scale of about λ. From (20), there will also be a wavelength-scale decorrelation in $g_{ss}^{(1)}(\Delta\mathbf{r})$, an observation that is supported by experimental data [32]. There is also a long range correlation where the light interacts with the object and a translated version at shared points, as Fig. 1 shows, and this forms a representation for macroscopic imaging. Therefore, we write

$$g_{ss}^{(1)}(\Delta\mathbf{r}) = g_{ss}^{(1)s}(\Delta\mathbf{r}) + g_{ss}^{(1)l}(\Delta\mathbf{r}), \tag{40}$$

where $g_{ss}^{(1)s}$ is the short-range correlation, with $|\Delta\mathbf{r}| \sim \lambda$, and $g_{ss}^{(1)l}$ is the long-range correlation (assuming $D > \lambda$, referring to Fig. 3) that exists because the deterministic moving object modifies the background field at each point in space within the joint spatial support of the scatterer and the translated scatterer (see Fig. 1). We have experimental evidence that both $g_{ss}^{(1)s}(\Delta\mathbf{r})$ and $g_{ss}^{(1)l}(\Delta\mathbf{r})$ can be observed with heavily scattered light [32].

We consider now forms of (39) in the large and small translation distance regimes, relative to λ, and in the weak and strong scatter contrast domains. This set of delineations relates to various application domains for the theory.

A. $|\Delta\mathbf{r}| \gg \lambda$

With $|\Delta\mathbf{r}| \gg \lambda$, and from (22), we assume that $g_{bs}^{(1)}(\Delta\mathbf{r}) = 0$ and $g_{ss}^{(1)s}(\Delta\mathbf{r}) = 0$. Normalization yields $g_{ss}^{(1)}(0) = 1$ but $g_{ss}^{(1)l}(0) \neq 1$. In this situation of large object translation relative to λ, we have from (39)

$$\begin{aligned}\langle \tilde{I}_d(\mathbf{r}_0)\tilde{I}_d(\mathbf{r}_0+\Delta\mathbf{r})\rangle = C_0^l(\Delta\mathbf{r};\mathbf{r}_0) + 2\Re\left\{C_1^{l*}(\Delta\mathbf{r};\mathbf{r}_0)g_{ss}^{(1)l}(\Delta\mathbf{r})\right\} \\ +C_2(\Delta\mathbf{r};\mathbf{r}_0)|g_{ss}^{(1)l}(\Delta\mathbf{r})|^2, \end{aligned} \tag{41}$$

with

$$\begin{aligned} C_0^l(\Delta\mathbf{r};\mathbf{r}_0) = \langle I_d(\mathbf{r}_0)\rangle^{-1}\langle I_d(\mathbf{r}_0+\Delta\mathbf{r})\rangle^{-1}\Big\{\langle I_{db}\rangle^2 + \langle I_{db}\rangle^{3/2}\langle I_{ds}(\mathbf{r}_0)\rangle^{1/2}2\Re\{g_{bs}^{(1)}(0)\} \\ +\langle I_{db}\rangle\langle I_{ds}(\mathbf{r}_0)\rangle\Big\} \end{aligned} \tag{42}$$

$$\begin{aligned} C_{1r}^l(\Delta\mathbf{r};\mathbf{r}_0) &= C_{12}(\Delta\mathbf{r};\mathbf{r}_0)\Re\{g_{bs}^{(1)}(0)\} + C_{13}(\Delta\mathbf{r};\mathbf{r}_0) \\ C_{1i}^l(\Delta\mathbf{r};\mathbf{r}_0) &= -C_{12}(\Delta\mathbf{r};\mathbf{r}_0)\Im\{g_{bs}^{(1)}(0)\}, \end{aligned} \tag{43}$$

and with $C_{12}(\Delta\mathbf{r};\mathbf{r}_0)$ and $C_{13}(\Delta\mathbf{r};\mathbf{r}_0)$ from (36).

B. $|\Delta\mathbf{r}| < \lambda$

Given a sufficiently small scan distance, we assume that stationarity holds, leading to $\langle I_d(\mathbf{r}_0)\rangle \approx \langle I_d(\mathbf{r}_0+\Delta\mathbf{r})\rangle$ and $\langle I_{ds}(\mathbf{r}_0)\rangle \approx \langle I_{ds}(\mathbf{r}_0+\Delta\mathbf{r})\rangle$. This approximation also holds with larger scan distance and sufficient background random scatter. Therefore, in conjunction with (39), we have

$$\begin{aligned} C_0(\Delta\mathbf{r};\mathbf{r}_0) = \langle I_d(\mathbf{r}_0)\rangle^{-2}\Big\{&\langle I_{db}\rangle^2 \\ &+ 2\langle I_{db}\rangle^{3/2}\langle I_{ds}(\mathbf{r}_0)\rangle^{1/2}\left[\Re\{g_{bs}^{(1)}(\Delta\mathbf{r})\} + \Re\{g_{bs}^{(1)}(0)\}\right] \\ &+ \langle I_{db}\rangle\langle I_{ds}(\mathbf{r}_0)\rangle 2\Re\{g_{bs}^{(1)}(0)g_{bs}^{(1)}(\Delta\mathbf{r})\} \\ &+ \langle I_{db}\rangle\langle I_{ds}(\mathbf{r}_0)\rangle\left[1+|g_{bs}^{(1)}(\Delta\mathbf{r})|^2\right]\Big\} \\ C_{1r}(\Delta\mathbf{r};\mathbf{r}_0) = C_{11}(\mathbf{r}_0)\Re\{g_{bs}^{(1)}(\Delta\mathbf{r})\} &+ C_{12}(\mathbf{r}_0)\Re\{g_{bs}^{(1)}(0)\} + C_{13}(\mathbf{r}_0) \\ C_{1i}(\Delta\mathbf{r};\mathbf{r}_0) = C_{11}(\mathbf{r}_0)\Im\{g_{bs}^{(1)}(\Delta\mathbf{r})\} &- C_{12}(\mathbf{r}_0)\Im\{g_{bs}^{(1)}(0)\} \\ C_2(\mathbf{r}_0) = \langle I_d(\mathbf{r}_0)\rangle^{-2}&\langle I_{ds}(\mathbf{r}_0)\rangle^2, \end{aligned} \tag{44}$$

where C_{11}, C_{12}, C_{13} and C_2, defined in (36), are now assumed independent of scan distance over the scale of one wavelength. Consequently,

$$\begin{aligned} C_{11}(\mathbf{r}_0) &= C_{12}(\mathbf{r}_0) \\ &= \langle I_d(\mathbf{r}_0)\rangle^{-2}\langle I_{db}\rangle^{1/2}\langle I_{ds}(\mathbf{r}_0)\rangle^{3/2} \\ C_{13}(\mathbf{r}_0) &= \langle I_d(\mathbf{r}_0)\rangle^{-2}\langle I_{db}\rangle\langle I_{ds}(\mathbf{r}_0)\rangle \end{aligned} \tag{45}$$

We note that it is of significance that measurements in this regime with heavy background random scatter could result in far-subwavelength information. This could be obtained from $g_{bs}^{(1)}(\Delta\mathbf{r})$, which varies with the object function. It is also available from $g_{ss}^{(1)s}$ and from (39).

C. $\langle I_{db}\rangle \gg \langle I_{ds}\rangle$

If the scattering object, large or small, is weakly scattering so that $\langle I_{ds}\rangle \ll \langle I_{db}\rangle$, we can approximate (39) as

$$\langle \tilde{I}_d(\mathbf{r}_0)\tilde{I}_d(\mathbf{r}_0+\Delta\mathbf{r})\rangle = C_0(\Delta\mathbf{r};\mathbf{r}_0) + 2\Re\left\{C_1^*(\Delta\mathbf{r};\mathbf{r}_0)g_{ss}^{(1)}(\Delta\mathbf{r})\right\}, \tag{46}$$

with

$$C_0(\Delta\mathbf{r};\mathbf{r}_0) = 1 + \frac{\left[\langle I_{ds}(\mathbf{r}_0+\Delta\mathbf{r})\rangle^{1/2}2\Re\{g_{bs}^{(1)}(\Delta\mathbf{r})\} + \langle I_{ds}(\mathbf{r}_0)\rangle^{1/2}2\Re\{g_{bs}^{(1)}(0)\}\right]}{\langle I_{db}\rangle^{1/2}}. \tag{47}$$

D. $\langle I_{db}\rangle \ll \langle I_{ds}\rangle$

With $\langle I_{db}\rangle \ll \langle I_{ds}\rangle$ and (39), we have the approximation

$$\langle \tilde{I}_d(0)\tilde{I}_d(\Delta\mathbf{r})\rangle = \left|g_{ss}^{(1)}(\Delta\mathbf{r})\right|^2. \tag{48}$$

VIII. SENSING AND IMAGING METHODOLOGY

A. Formation of Averages ($\langle\cdot\rangle$) with Experimental Data

The averaging process in our theory, $\langle\cdot\rangle$, is mathematically an average over background scatterer reconfiguration. This means in forming $\langle \tilde{I}_d(\mathbf{r}_0)\tilde{I}_d(\mathbf{r}_0+\Delta\mathbf{r})\rangle$ that the intensity is

measured at the detector point ($\mathbf{r}_d$) with the object at $\mathbf{r}_0$ (giving the p-th measurement as $I_{dp}(\mathbf{r}_0)$) and at $\mathbf{r}_0+\Delta\mathbf{r}$ (resulting in $I_{dp}(\mathbf{r}_0+\Delta\mathbf{r})$). Upon rearranging the background scatters according to a relevant density function, a set of random samples is obtained. Thus, the average with P measurements is formed as $\langle\tilde{I}_d(0)\tilde{I}_d(\Delta\mathbf{r})\rangle = \frac{1}{P}\sum_{p=1}^{P}\tilde{I}_{dp}(0)\tilde{I}_{dp}(\Delta\mathbf{r})$, with P suitably large. It is not practical to form averages involving rearrangement of the background scatterers experimentally, because the object of interest would need to be in two locations for each measurement with the background scatterer configuration being identical.

Experimentally, one can estimate $\langle\cdot\rangle$ using a camera image of the speckle intensity where the image domain is small enough for stationary statistics to hold [6, 31–33]. In this case, each speckle spot needs to be adequately resolved, there needs to be a sufficient number of spots, and the regions imaged onto the camera should be small enough for the mean to be independent of position within a given image (but not necessarily as $\Delta\mathbf{r}$ is varied). Thus, the average is formed over the pixels of a camera. The requirement for independent samples can be met with a sufficient number of speckle spots. The sampling can be enhanced by using multiple reference positions ($\mathbf{r}_p$) and equivalent offsets ($\Delta\mathbf{r}$) [33]; this has also been done to form an average over frequency [6]. The normalized intensity images associated with each measurement can thus be formed.

B. $\langle I_{db}\rangle = 0$: Aperture in a Screen

The simplest case corresponds to an aperture in a screen, where, with the object absent, there is no field on the detector side for a transmission measurement. In this situation, (48) is exact. This has been the basis of imaging results presented using experimental data [32].

C. $\langle I_{db}\rangle \neq 0$: General Object

We consider the heavy scatter regime and $\Delta\mathbf{r} \gg \lambda$, allowing us to write (41) as

$$\langle\tilde{I}_d(\mathbf{r}_0)\tilde{I}_d(\mathbf{r}_0+\Delta\mathbf{r})\rangle = C_0^l(\mathbf{r}_0) + 2\Re\left\{C_1^{l*}(\mathbf{r}_0)g_{ss}^{(1)l}(\Delta\mathbf{r})\right\} + C_2(\mathbf{r}_0)|g_{ss}^{(1)l}(\Delta\mathbf{r})|^2, \qquad (49)$$

where within a scan distance corresponding to the joint support of the object and its translated self, it has been found that C_0^l, C_1^{l*}, and C_2 can be treated approximately as constants [33]. The measured intensity data as a function of object position is then related to four real numbers and $g_{ss}^{(1)l}$, the object autocorrelation function. In principle, (49) can be solved and

$g_{ss}^{(1)l}(\Delta\mathbf{r})$ obtained. Then, through a Gerchberg-Saxton [36] phase reconstruction process (see [37, 38], for example), the object function $\tilde{O}$ can be retrieved from $g_{ss}^{(1)l}(\Delta\mathbf{r})$ based on (28) [32, 33].

Experiments with a translated millimeter-scale absorbing patch (formed with black tape) in a heavily scattering background have found C_1 to be small [33]. Consequently, in such situations, where the second term in (49) is small, C_0^l can be extracted from measured data, and (49) can be renormalized so that $|g_{ss}^{(1)l}(0)| = 1$. These steps provide direct access to the normalized object autocorrelation function from (28). In a general situation where the second term in (49) cannot be neglected, optimization-based fitting can provide the three constants and hence access to the object autocorrelation.

IX. APPLICATIONS AND PERSPECTIVES

Our compact, central result in (39) provides a new and fundamental description of intensity correlations over (moving object) space that persist over infinite length scales. In practice, the distances and levels of scatter become limited by the laser source energy and detector noise. Previous investigations into second order intensity correlations (see Refs. [5, 39–42] for a review) have identified contributors to the measured intensity correlation of $C_I(\Delta x) = \langle I(x_0)I(x_0 + \Delta x)\rangle$, where Δx represents the change in the correlation variable (e.g., frequency or wave-vector direction) and the brackets $\langle\cdots\rangle$ represent the ensemble average. $C_I(\Delta x)$ has been decomposed into three terms, short-range correlations $C_1(\Delta x)$, long-range correlations $C_2(\Delta x)$, and infinite-range correlations $C_3(\Delta x)$ [17] (where we preserve the notation in the cited reference, but note that the definitions of C_1 and C_2 are not the same as in the development given in this work). Each of these correlations may contribute to the measured correlation, and they have been weighted by the dimensionless quantity g (dimensionless conductance) according to $C_I(\Delta x) = C_1(\Delta x) + g^{-1}C_2(\Delta x) + g^{-2}C_3(\Delta x)$. For most optical experiments involving a slab geometry, $g \gg 1$ is typical, thus making the contribution of the long- and infinite-range correlations negligible [43]. Our work with correlations over object position provides another infinite range correlation for situations that pertain to a randomly scattering slab where the thickness can in principle approach infinity.

A number of fundamental assumptions were made in the development of our theory that impact applications: we assume that the statistics from a set of camera images will be a

good indicator of an average formed from rearrangements of the environmental scatterers; there is natural or controlled motion of the object of interest; the background scattering environment is assumed to be static within the acquisition of speckle images; and, most importantly, we have stipulated that the statistics of the detected speckle field to exhibit a circular Gaussian distribution, required for use of Reed's moment theorem [7]. We address each of these requirements.

In an experiment, averages would be formed with camera speckle images that access random intensity information over space (or angle). The statistics from the camera image are expected to be a good representation provided each speckle is spatially resolved and there are enough independent samples. Our experience with reasonably heavily scattering media is that a spot of about 1 mm in diameter can have approximately a constant mean intensity, thereby providing stationary statistics in the camera image [6, 8, 30–32, 44, 45]. A 4-F lens system with an aperture in the Fourier domain provides separate control of the speckle size. There is a trade-off between speckle size and number of speckle spots, where the camera pixel size should be small relative to the speckle (autocorrelation function full width half maximum) and there should be a sufficient number (of independent samples) within an image where the statistics are stationary (so the mean is constant). Measurements are made through a polarizer. Negative exponential intensity statistics indicate that the speckle images are satisfactory and that the fields are zero-mean-circular Gaussian. Laser light with adequate coherence is also required (to achieve satisfactory statistics), and this requirement is a function of the amount of background scatter.

Various physical situations involve object motion. One example is *in vivo* blood vessel constituents. In other applications, motion could be induced using a translational stage. This may be appropriate in material inspection, for instance. Regardless, prior information on the motion of the object during the acquisition of speckle images is needed to apply this approach which means the positional or velocity information of the unknown moving object needs to be inferred through some complementary method, such as temporal decorrelation or the Doppler shift [46], or localization based on a photon diffusion model [47]. The dimensionality of any sensing and imaging result is commensurate with that of the object motion. For motion other than linear translation, we foresee that a similar type of theory may be possible. Given enough prior information about the motion of the object, the experimentally-measured correlation could potentially be separated to different types of

object motion, such as translation and rotation, and analyzed for useful sensing and imaging.

The need for stationary (static) background scatterer positions is perhaps the most severe restriction. Natural settings may involve motion of the scatterers, such as with aerosols. It is assumed that displacement of background scatterers with the motion of the object of interest can be neglected. Generally, the stationary background scatterer requirement implies that this motion is negligible during the measurement period over which the object is moving. Alternatively, the implication is that intensity decorrelation due to the motion of the randomly located background scatterers can be accounted for in a calibration and hence known from prior information. This constraint also relates to object size or speed, which has a detector signal-to-noise ratio implication.

An amount of scatter producing developed Gaussian field statistics is assumed. This assumption can be met with a random medium having a thickness of one transport length, the distance for photon momentum randomization, or more. Heavier scatter, such that the mean intensity does not vary appreciably with object position over the measurement, provides a simplification, and can lead to approximating C_0, C_1 and C_2 as constant for $\Delta\mathbf{r}$ about the moving object's size in our development in Sect. VIII.

We have been able to reconstruct images of macroscopic (mm-scale) objects, both apertures of rather complex shapes and also black patches by obtaining speckle images as a function of translated object position and applying the theory of Sect. VIII [33]. This was achieved by assuming that C_0, and C_2 are constants that can be determined by fitting the measured data and assuming $C_1 = 0$ [33]. This provided access to $g_{ss}^{(1)l}$ and hence the object autocorrelation, from which phase retrieval allowed imaging of the object to quite high precision. The principle is that correlations exist within the joint support and the wavelength-scale correlation, $g_{ss}^{(1)s}$, is neglected. In the general situation where these coefficients are spatially dependent, inversion becomes ill-posed. Consequently, prior information would be needed or constraints imposed. Recently, we have also obtained experimental results that support using the ratio between C_0^l and C_2^l in (49) to qualitatively compare the relative scattering strengths of the moving object and the scattering environment. This suggests that various measures based on our general result in (39) could be of practical importance. While the resolution could in principle approach wavelength scale in this macroscopic regime, in practice it is limited by scanning precision and other practical aspects of making such measurements.

The experimental evidence for super-resolution sensitivity in a speckled field is compelling [32]. This subwavelength length-scale information is contained within $g_{ss}^{(1)}$, specifically $g_{ss}^{(1)s}(\Delta\mathbf{r})$, and likely $g_{bs}^{(1)}(\Delta\mathbf{r})$ (although there is currently no experimental information relevant to the character of $g_{bs}^{(1)}(\Delta\mathbf{r})$). A combined numerical field study and the pursuit of experiments with nanoparticles could shed light on these functions and may provide a means to extract object parameters of relevance, hence providing sensing and perhaps even imaging on this length scale. The achievement of far-subwavelength object information with motion in a speckled field is analogous to an earlier proposal for motion in structured illumination achieved by two interfering beams [29]. The distinction in the case of the speckled field is that the field is generally unknown and hence a forward model and conventional computational imaging approaches cannot be applied.

More generally, our method could allow communication in a cluttered environment. Consider a moving transmitter that sends an identical set of signals from a series of spatial positions. This information could in principle be extracted in a manner similar to how imaging is accomplished. Again, the principle is correlated information that survives the averaging process with multiply-scattered light. In this case, temporal or multiple frequency data would be extracted. There are of course details to be investigated as to how a protocol for this communication arrangement would be implemented, but the principle we have described should be applicable. This may also carry over to quantum key distribution in the presence of clutter [48].

Ghost imaging involves entangled or correlated photons [49]. Speckle can occur [50] and achieving high contrast-to-noise control is important [51, 52]. It may be possible to utilize object motion to enhance the robustness of ghost imaging in a scattering environment. In fact, moving objects have been considered in ghost imaging [53] and this could be extended to heavily scattering media with our approach. With regard to energy-time entangled photons in scattering media, correlated detection (in the Hanbury Brown and Twiss sense) or detection with a nonlinear crystal [54] provides temporal gating that could be useful in scattering media. With a moving entangled photon source in a scattering medium, information can be added by position control that could be interesting in applications.

Finally, fluorescence (or Förster) resonance energy transfer (FRET) is a non-radiative energy transfer process between donor and acceptor molecules spatially separated by a distance usually between 1-10 nm that results in a decrease in the lifetime and quantum yield

of the donor in the presence of the acceptor [55]. Measurement of FRET through lifetime modification has become important in molecular biology [56] and has been shown possible for *in vivo* applications [57, 58]. With suitable labeling, FRET can provide key information about protein folding, relevant for many major diseases. Generally, the change of lifetime is represented as a donor-acceptor distance using classical dipole-dipole coupling theory [55]. It may be possible to use a coherent method based on absorption and motion along the lines we have described to separately determine the distance (which is typically several nanometers).

X. CONCLUSION

We have presented a rigorous theory for imaging based on speckle pattern correlations over object position. This leads to various sensing and imaging opportunities using coherent light in scattering media. It may be possible to exploit natural motion in environmental sensing situations where multiple scatter occurs. If the motion of the object of interest were fast relative to the background scattering medium, then the situation would conform to the theory described. It may also be possible to calibrate for decorrelation due to the background, provided there is adequate sensitivity to the moving object to be imaged. An important application domain is *in vivo* imaging without contrast agents, such as of blood cells in capillaries. In this case, the local velocity may be constant over the micron length scales required. While the corresponding translation is 1D, 3D imaging may be possible with constraints. Accessing far-subwavelength information is an intriguing direction. This is relevant in finding defects in semiconductor device processing using optical inspection. The wafer can be precisely positioned but traditional methods are diffraction-limited and hindered by speckle produced due to surface roughness and complicated 3D structures. It is possible that the presence of defects may be determined by using speckle intensity correlation over the wafer position. In weakly scattering situations, such as in microscopy where super-resolution would be value, the speckle could be created by a diffusing screen and the object of interest (cells for example) translated in this structured field, allowing intensity images to be captured as a function of object position.

XI. ACKNOWLEDGMENTS

This work was supported by the National Science Foundation under grants 1610068 and 1618908, by the Air Force Office of Scientific Research under grant FA9550-19-1-0067, and by the Laboratory Directed Research and Development (LDRD) and Sandia Academic Alliance (SAA) Programs at Sandia National Laboratories. Sandia National Laboratories is a multimission laboratory managed and operated by National Technology and Engineering Solutions of Sandia, LLC, a wholly owned subsidiary of Honeywell International Inc., for the U.S. Department of Energy's National Nuclear Security Administration under contract DE-NA0003525."

---

[1] J. W. Goodman, *Statistical Optics* (New York, Wiley-Interscience, 1985).

[2] D. J. Pine, D. A. Weitz, P. M. Chaikin, and E. Herbolzheimer, Phys. Rev. Lett. **60**, 1134 (1988).

[3] A. Fercher and J. Briers, Opt. Commun. **37**, 326 (1981).

[4] A. K. Dunn, H. Bolay, M. A. Moskowitz, and D. A. Boas, J. Cereb. Blood Flow Metab. **21**, 195 (2001).

[5] J. H. Li and A. Z. Genack, Phys. Rev. E **49**, 4530 (1994).

[6] M. A. Webster, K. J. Webb, and A. M. Weiner, Phys. Rev. Lett. **88**, 033901 (2002).

[7] I. S. Reed, IRE Trans. Inform. Theory **8**, 194 (1962).

[8] J. D. McKinney, M. A. Webster, K. J. Webb, and A. M. Weiner, Opt. Lett. **25**, 4 (2000).

[9] B. Redding, M. A. Choma, and H. Cao, Nat. Photon. **6**, 355 (2012).

[10] Y. Bromberg and H. Cao, Phys. Rev. Lett. **112**, 213904 (2014).

[11] A. L. Moustakas, H. U. Baranger, L. Balents, A. M. Sengupta, and S. H. Simon, Science **287**, 287 (2000).

[12] F. Lemoult, G. Lerosey, J. de Rosny, and M. Fink, Phys. Rev. Lett. **103**, 173902 (2009).

[13] R. Pappu, B. Recht, J. Taylor, and N. Gershenfeld, Science **297**, 2026 (2002).

[14] J. F. Barrera, R. Henao, M. Tebaldi, R. Torroba, and N. Bolognini, Opt. Commun. **276**, 231 (2007).

[15] B. Redding, S. F. Liew, R. Sarma, and H. Cao, Nat. Photon. **7**, 746 (2013).

[16] A. Z. Genack, Phys. Rev. Lett. **58**, 2043 (1987).

[17] S. Feng, C. Kane, P. A. Lee, and A. D. Stone, Phys. Rev. Lett. **61**, 834 (1988).

[18] I. Freund, M. Rosenbluh, and S. Feng, Phys. Rev. Lett. **61**, 2328 (1988).

[19] I. Freund, Physica A **168**, 49 (1990).

[20] J. Bertolotti, E. G. van Putten, C. Blum, A. Lagendijk, W. Vos, and A. P. Mosk, Nature **491**, 232 (2012).

[21] O. Katz, E. Small, and Y. Silberberg, Nat. Photon. **6**, 549 (2012).

[22] O. Katz and S. Gigan, Nat. Photon. **8**, 784 (2014).

[23] I. M. Vellekoop and A. P. Mosk, Opt. Lett. **32**, 2309 (2007).

[24] R. Horstmeyer, H. Ruan, and C. Yang, Nat. Photon. **9**, 563 (2015).

[25] S. Popoff, G. Lerosey, M. Fink, A. C. Boccara, and S. Gigan, New J. Phys. **13**, 123021 (2011).

[26] A. Mosk, A. Lagendijk, G. Lerosey, and M. Fink, Nat. Photon. **6**, 283 (2012).

[27] T. Chaigne, O. Katz, A. C. Boccara, M. Fink, E. Bossy, and S. Gigan, Nat. Photon. **8**, 58 (2013).

[28] M. Davy, Z. Shi, and A. Z. Genack, Phys. Rev. B **85**, 035105 (2012).

[29] K. J. Webb, Y. Chen, and T. A. Smith, Phys. Rev. Appl. **6**, 024020 (2016).

[30] J. A. Newman and K. J. Webb, Opt. Lett. **37**, 1136 (2012).

[31] J. A. Newman and K. J. Webb, Phys. Rev. Lett. **113**, 263903 (2014).

[32] J. A. Newman, Q. Luo, and K. J. Webb, Phys. Rev. Lett. **116**, 73902 (2016).

[33] Q. Luo, J. A. Newman, and K. J. Webb, Opt. Lett. **44**, 2716 (2019).

[34] A. J. F. Siegert, *MIT Rad Lab Rep No 465* (1943).

[35] M. A. Webster, K. J. Webb, A. M. Weiner, J. Xu, and H. Cao, J. Opt. Soc. Am. A **20**, 2057 (2003).

[36] R. Gerchberg and W. Saxton, Optik **35**, 227 (1972).

[37] J. R. Fienup, Appl. Opt. **21**, 2758 (1982).

[38] J. A. Rodriguez, R. Xu, C. C. Chen, Y. Zou, and J. Miao, J. Appl. Crystallogr. **46**, 312 (2013).

[39] P. Sheng, *Scattering and Localization of Classical Waves in Random Media*, Vol. 8 (World Scientific Pub Co Inc, 1990).

[40] S. Feng and P. A. Lee, Science **251**, 633 (1991).

[41] R. Berkovits and S. Feng, Phys. Rep. **238**, 135 (1994).

[42] M. C. W. van Rossum and T. M. Nieuwenhuizen, Rev. Mod. Phys. **71**, 313 (1999).

[43] F. Scheffold, W. Hartl, G. Maret, and E. Matijevic, Phys. Rev. B **56**, 10942 (1997).

[44] Z. Wang, M. A. Webster, A. M. Weiner, and K. J. Webb, J. Opt. Soc. Am. A **23**, 3045 (2006).

[45] Z. Wang, K. J. Webb, and A. M. Weiner, Appl. Opt. **49**, 5899 (2010).

[46] J. D. Briers, Physiol. Meas. **22**, R35 (2001).

[47] B. Z. Bentz, T. C. Wu, V. Gaind, and K. J. Webb, Appl. Opt. **56**, 6649 (2017).

[48] P. W. Shor and J. Preskill, Phys. Rev. Lett. **85**, 441 (2000).

[49] D. V. Strekalov, A. V. Sergienko, D. N. Klyshko, and Y. H. Shih, Phys. Rev. Lett. **74**, 3600 (1995).

[50] F. Ferri, D. Magatti, A. Gatti, M. Bache, E. Brambilla, and L. A. Lugiato, Phys. Rev. Lett. **94**, 183602 (2005).

[51] K. W. C. Chan, M. N. O'Sullivan, and R. W. Boyd, Opt. Lett. **34**, 3343 (2009).

[52] K. W. C. Chan, D. S. Simon, A. V. Sergienko, N. D. Hardy, J. H. Shapiro, P. B. Dixon, G. A. Howland, J. C. Howell, J. H. Eberly, M. N. O'Sullivan, B. Rodenburg, and R. W. Boyd, Phys. Rev. A **84**, 043807 (2011).

[53] S. Sun, H. Lin, Y. Xu, J. Gu, and W. Liu, Opt. Express **27**, 27851 (2019).

[54] F. Zäh, M. Halder, and T. Feurer, Opt. Express **16**, 16452 (2008).

[55] T. Förster, Ann. Physik **2**, 55 (1948).

[56] J. Zhang, R. E. Campbell, A. Y. Ting, and R. Y. Tsien, Nat. Rev. Mol. Cell Biol. **3**, 906 (2002).

[57] V. Gaind, S. Kularatne, P. S. Low, and K. J. Webb, Opt. Lett. **35**, 1314 (2010).

[58] E. H. Tsai, B. Z. Bentz, V. Chelvam, V. Gaind, K. J. Webb, and P. S. Low, Biomed. Opt. Express **5**, 2662 (2014).

FIGURES

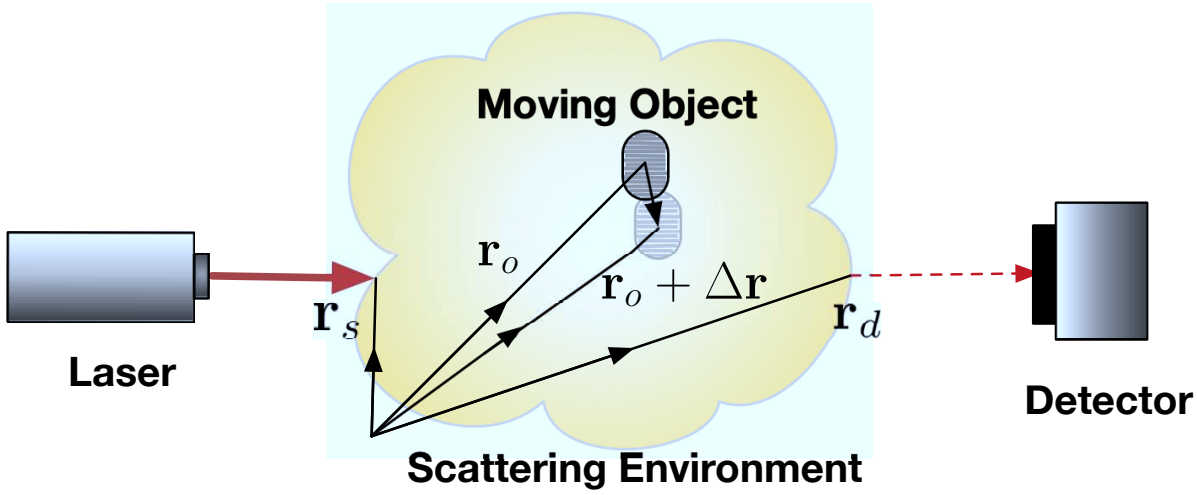

FIG. 1. A moving object in a scattering medium to be imaged, along with the spatial variables and the optical excitation and detection concept.

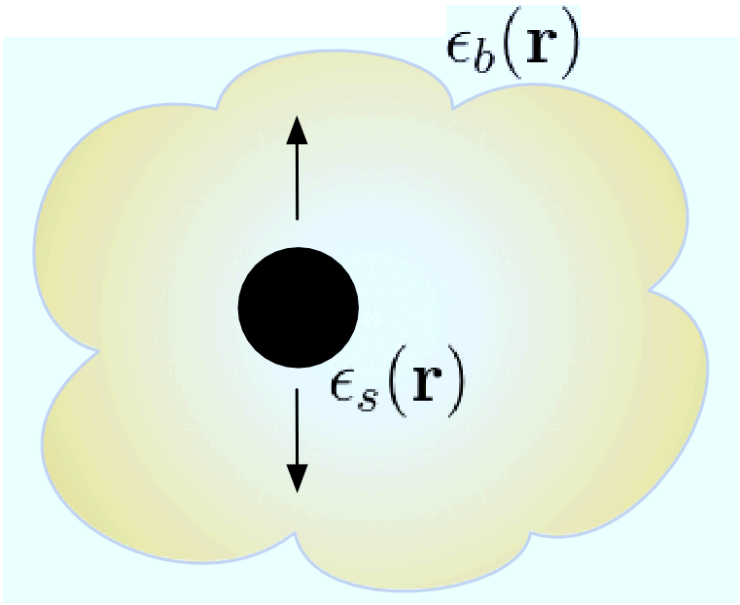

FIG. 2. The separation of a randomly scattering background, described by a spatial variation of the background dielectric constant, $\epsilon_b(\mathbf{r})$, and the moving object's dielectric constant, $\epsilon_s(\mathbf{r})$, allows separation of the fields and facilitates the development of (39).

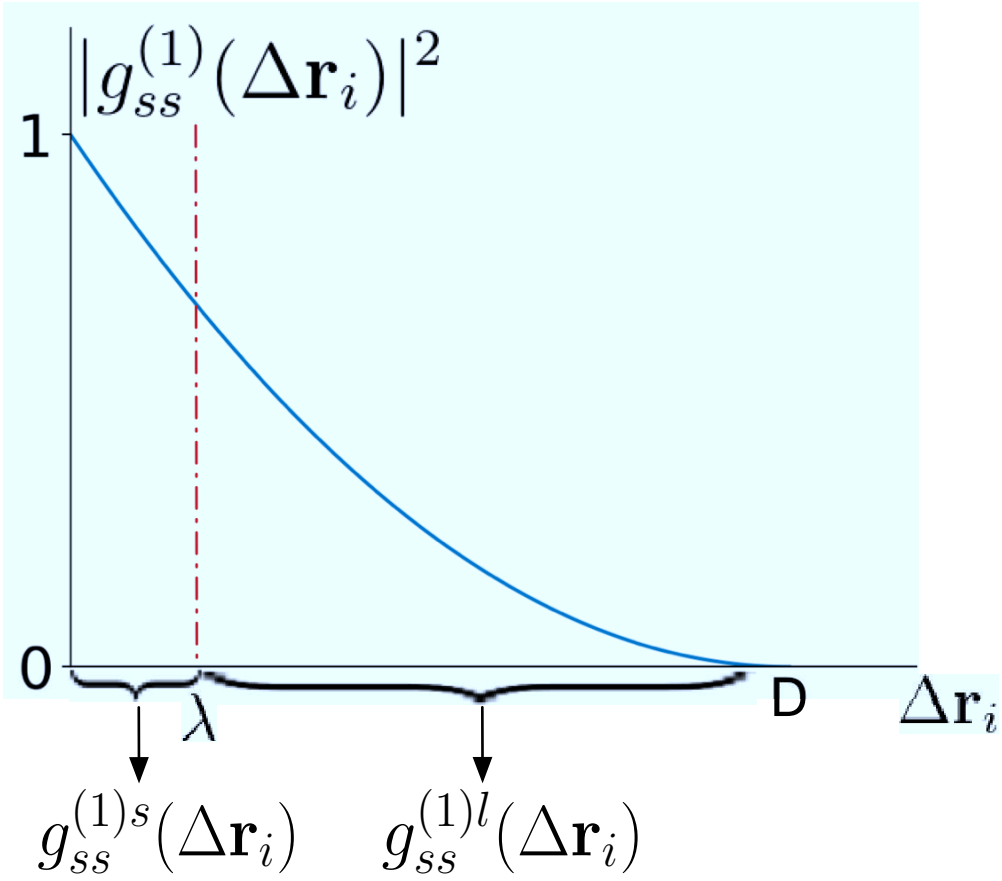

FIG. 3. The normalized scattered field correlation is shown to have a short-range, wavelength-scale regime, as well as a long range macroscopic object characteristic that goes to a minimum at a distance corresponding to the size of the object, D. This depiction is consistent with a relationship to the object autocorrelation function and experimental data [32, 33].